Graefe's Arch Clin Exp Ophthalmol (1985) 223:69–76

Graefe's Archive
for Clinical and Experimental
Ophthalmology

Senile macular degeneration: The involvement of immunocompetent cells

P.L. Penfold, M.C. Killingsworth, and S.H. Sarks
Department of Ophthalmology and Eye Research, Lidcombe Hospital, Joseph Street, Lidcombe, N.S.W. 2141, Sydney, Australia

Abstract. Senile macular degeneration (SMD) is a leading cause of legal blindness in western countries. The role of immunocompetent cells in the pathogenesis of this disease has not been widely recognised. In this work specimens were studied by electron microscopy to provide ultrastructural details of the role of immunocompetent cells in early, intermediate and late stages of the disease. Additionally, we have analysed the frequency and distribution of inflammatory cellular infiltrates using wax histology. The results illustrate the involvement of macrophage-series cells, fibroblasts, lymphocytes and mast cells in neovascularisation, atrophy of the retinal pigment epithelium and the breakdown of Bruch's membrane. These observations, together with previous clinicopathological studies, have led us to suggest that SMD has a chronic inflammatory component.

Introduction

Numerous recent surveys have shown that senile macular degeneration (SMD) is a leading cause of legal blindness in western countries (Lancet editorial, 1983; Ghafour et al. 1983; Sorsby 1966). Typically, SMD occurs in individuals 60 years and older. There is no sex predilection and degeneration is often bilateral. Early degenerative changes, including pigmentary disturbances and numerous drusen, may become apparent ophthalmoscopically. Loss of central vision develops either gradually as a result of atrophy of the retinal pigment epithelium, or rapidly following the complications of subretinal neovascularisation. The fundamental cause of these changes is unknown.

The degree of degeneration has been related histologically to the progressive accumulation of an abnormal basal laminar deposit beneath the pigment epithelium (Sarks 1976). Immunocompetent cells have not been considered to play a role in the pathogenesis of SMD; a previous publication, however, noted macrophage-like cells within Bruch's membrane (Grindle and Marshall 1978). More recently, histiocytic and giant cells have been observed in association with breaks in Bruch's membrane and subretinal neovascular membranes (Sarks et al. 1980; Killingsworth and Sarks 1982). Additionally, we have shown (Penfold et al. 1984) that inflammatory cells, including macrophages, fibroblasts and mast cells, play a role in the breakdown of Bruch's membrane.

Offprint requests to: P.L. Penfold, M.D.

This paper further illustrates the involvement of immunocompetent cells in neovascularisation, atrophy of the pigment epithelium and the breakdown of Bruch's membrane and suggests that SMD has an inflammatory component.

Materials and methods

The present study is based on ultrastructural and histological findings in 67 post-mortem eyes demonstrating all stages of macular degeneration. The eyes were taken from male and female patients whose ages at death ranged from 40 to 94 years. All patients, with the exception of the 40 year old, had been hospitalised for long-term care and a full ocular examination had been performed at intervals, including fundus photography and flourescein angiography, where indicated. Patients with blood dyscrasia or ocular disease that could have modified the cell population in the choroid were excluded. Eyes were enucleated within 6 h of death by a standard procedure.

For electron microscopy, seven eyes were fixed in 2.5% glutaraldehyde in 0.1 M cacodylate buffer (pH 7.4) at 4° C for 24 h. The specimens were then washed in 0.1 M cacodylate buffer (pH 7.4). The eyes were opened in the horizontal plane and an 8-mm corneal trephine was used to remove the posterior region, including the macula and optic nerve. The retina and choroid were dissected away from the sclera and the trephined disc was then further subdivided to produce blocks suitable for electron microscopy. The blocks were washed in fresh buffer and post-fixed in 2% osmium tetroxide in 0.1 M cacodylate buffer (pH 7.4) for 3 h, followed by 2% uranyl acetate staining for 1 h. Finally, the blocks were dehydrated in graded alcohols and acetone and embedded in Spurr's low-viscosity resin and cured for 8 h.

For light microscopy, eyes were fixed in Lillie's buffered formalin and serial sections 7 μm thick were cut horizontally through the disc and macula. Every tenth section was stained by the picro-Mallory method and three sections passing through the fovea were selected for each eye. Ten eyes were selected from each of six groups previously classified according to the light microscopical appearance of a laminar deposit at the base of the retinal pigment epithelial cells (Sarks 1976). Group I was considered to represent normal ageing, groups II, III and IV the progressive development of macular degeneration, and groups V and VI the end results of geographic atrophy of the pigment epithelium and disciform degeneration respectively. Ultrastructural examination of this material reveals the presence of numerous

Table 1. Cell counts in the blood vessels and stroma at the macula[a]

	Group I				Group II				Group III			
	ss	s	cc	c	ss	s	cc	c	ss	s	cc	c
1	2	50	8	22	8	178	33	41	9	115	20	26
2	0	29	17	11	9	301	31	91	6	187	17	36
3	0	21	21	11	0	92	18	34	2	83	30	53
4	0	13	18	26	1	120	54	47	8	101	37	23
5	0	21	24	30	5	59	37	43	6	108	46	71
6	0	34	31	45	0	52	32	40	5	117	55	26
7	0	13	19	36	5	70	31	30	3	184	44	141
8	2	32	10	11	2	76	30	19	3	63	15	21
9	0	40	22	29	1	59	40	26	2	37	21	23
10	0	36	53	31	3	15	20	19	8	62	48	106
Mean 50	0.4 ±0.52	28.9 ±11.94	22.3 ±12.6	25.2 ±11.5	3.4 ±3.2	102.2 ±82.51	32.6 ±10.1	39.0 ±28.7	5.2 ±2.6	105.7 ±49.3	32.3 ±14.5	53.6 ±41.43

	Group IV				Group V				Group VI			
	ss	s	cc	c	ss	s	cc	c	ss	s	cc	c
1	0	38	29	32	15	131	11	13	37	137	9	36
2	3	104	46	54	26	65	4	7	20	105	9	13
3	3	141	38	47	21	59	7	35	10	133	7	102
4	3	128	23	20	26	188	10	31	22	172	30	50
5	5	81	21	45	12	20	3	7	14	104	16	44
6	0	95	37	52	8	107	28	30	19	30	22	23
7	6	39	14	14	12	93	6	25	22	91	39	90
8	4	132	52	76	5	62	18	15	9	262	17	13
9	8	79	25	43	5	82	40	69	24	100	17	20
10	4	114	37	38	1	20	6	8	37	125	9	57
Mean 50	5.2 ±2.5	95.1 ±36.3	32.2 ±11.86	42.1 ±17.7	13.1 ±8.95	82.7 ±50.86	13.3 ±12.05	22.0 ±19.06	21.4 ±9.66	115.9 ±60.39	17.5 ±10.37	44.8 ±31.06

[a] Figures represent numbers of cells found within a standard area as described below:
ss–superficial stroma, i.e. within 10 μm of Bruch's membrane, area counted = 0.024 mm^2
s–stroma, i.e. 10–100 μm of Bruch's membrane, area counted = 0.219 mm^2
cc–choriocapillaris, i.e. within blood vessels within 10 μm of Bruch's membrane, area counted = 0.024 mm^2
c –choroid, i.e. within blood vessels 10–100 μm of Bruch's membrane, area counted = 0.219 mm^2
↓ –specimen number

Fig. 1. Illustrating the normal appearance of the RPE, Bruch's membrane (*B*), the choroid (*C*) and the choroidal stroma (*CS*) in a 40-year-old patient. (×1,680 final magnification)

Fig. 2. From a 62-year-old group-II patient illustrating the appearance of lymphocytes (*L*) and fibroblasts (*F*) in the stroma during the early phases of SMD. (×1,440 final magnification)

Fig. 3. A fibroblast (*F*) from a 75-year-old group-IV patient, associated with the outer surface of Bruch's membrane (*B*) beneath a drusen (*D*). (×4,500 final magnification)

Fig. 4. From the same patient as Fig. 3, illustrating the involvement of lymphocytes (*L*) in the intermediate phases of SMD. (×1,960 final magnification)

Fig. 5. A light micrograph from a 0.5 μm toluidene-blue stained section illustrating geographic atrophy in an 82-year-old patient. A giant cell (*G*) is shown closely applied to the inner surface of Bruch's membrane (*B*). It is surrounded by degenerated pigmented material (↓). The RPE is entirely atrophied (*A*). Numerous leucocytes and fibroblasts are scattered throughout the choroid (*C*↓). (×344 final magnification)

Fig. 6. A light micrograph from a 0.5 μm toluidene-blue stained section, illustrating disciform degeneration in a 72-year-old patient. The RPE is entirely atrophied and has been replaced by a layer of fibrous tissue (*F*). Numerous breaks have developed in Bruch's membrane (↓) and a new choroidal vessel is seen passing through into the fibrous layer (*NV*→). (See Fig. 7 below for EM view.) A more fully developed new vessel is apparent close to the fibrous tissue (↓*NV*). Red blood cells possibly derived from haemorrhage (*H*) of new vessels are apparent in the outer retinal layers. (×220 final magnification)

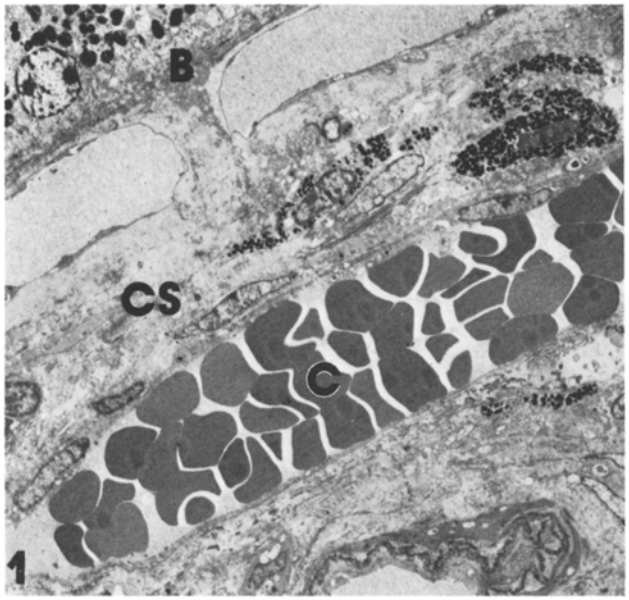
B
CS
C
1

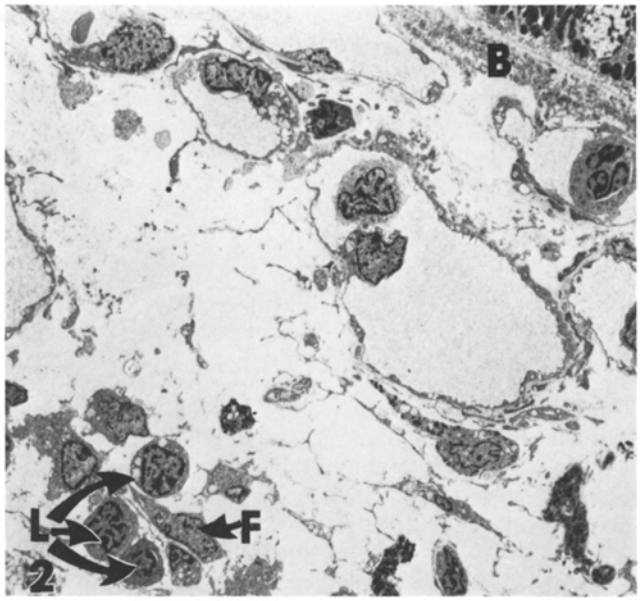
B
L
F
2


D
B
F
3


B
L
L
4

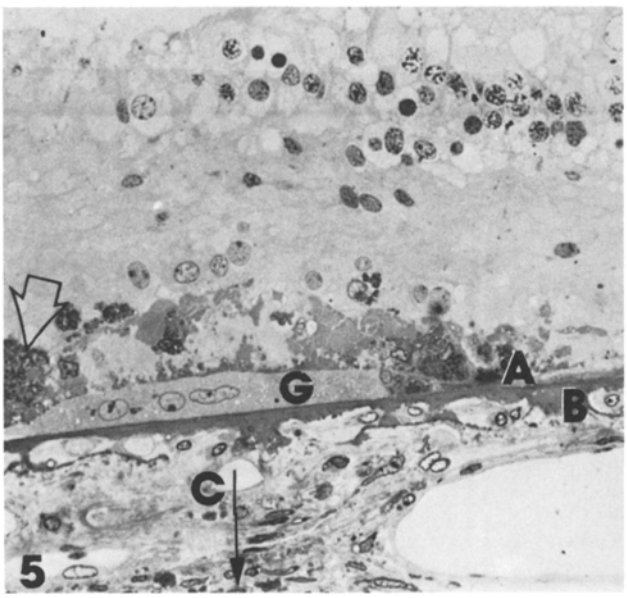
G
A
B
C
5

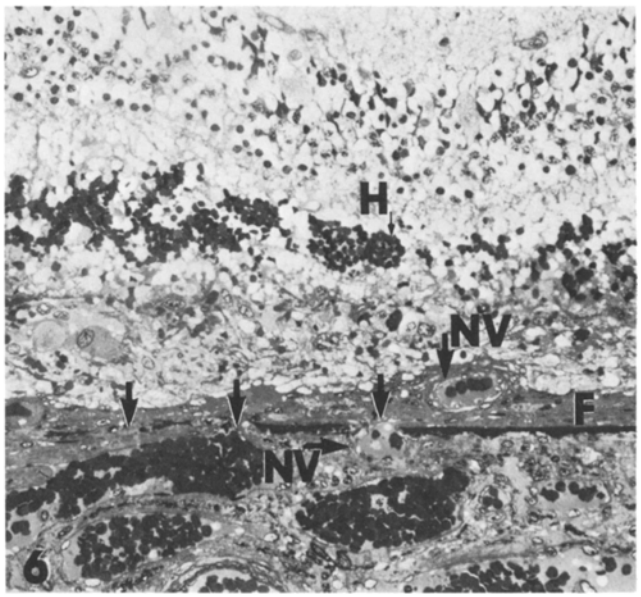
H
NV
F
NV
6

cell types, including lymphocytes, macrophage-series cells, granulocytes, fibrovascular components and melanocytes in the choroid at the macular. Due to the limitations of sample size inherent in ultrastructural studies, counts to assess the overall degree of cellular infiltration were made at the light microscopic level on wax-embedded material for each group. For this purpose all nucleated cells, excluding melanocytes, endothelial cells and pericytes, were included in the count. This approach provided an overview of cell number and their distribution in the groups (I–VI) whilst minimising the complications of tabulation and statistical analysis. Nucleated cells which were clearly intravascular, that is completely enclosed by vascular endothelium and in association with red blood cells, were counted separately. Figures 13–15 provide an impression of the level of detail available in these specimens. It should be pointed out that during the actual counting the coloured stain employed and focus variability made counting easier. The study was performed 'blind' on masked slides using a X40 objective lens and a X12.5 eye piece at a final magnification of X500. Using a calibrated eye-piece graticule to define the area to be counted, intravascular and extravascular cells were classed into four groups. Cells within blood vessels within 10 μm of Bruch's membrane were assigned to the choriocapillaris group (cc). Cells in the stroma within 10 μm of Bruch's membrane were assigned to the superficial stroma group (ss). Cells within blood vessels between 10 μm and 100 μm of Bruch's membrane were assigned to the choroid group (c). Cells in the stroma between 10 μm and 100 μm of Bruch's membrane were assigned to the stroma group (s). The results are presented in Table 1.

Results

The photomicrographs, numbered 1–12, are taken from seven eyes from seven patients selected to illustrate the histopathological features apparent at early, intermediate and late phases of SMD. Detailed descriptions of each figure are provided in the accompanying legends. The normal appearance of the choroidal stroma and vasculature is shown in Fig. 1. Low numbers of leucocytes and fibroblasts are normally present in the choroidal stroma, but they are not considered to be pathological.

An example of the appearance of inflammatory cells in the early stages of the disease is given in Fig. 2. Clusters of lymphocytes, monocytes and fibroblasts were frequently seen in the stroma. At this stage inflammatory cells were mainly observed in the stroma and not the superficial stroma. There was a significant correlation between numbers of cells in the stroma and numbers of cells in the choroidal vasculature (see results below).

Examples of the intermediate phase of the disease are provided in Figs. 3 and 4. Monocytes and fibroblasts were found apposed to the outer surface of Bruch's membrane in association with long-spacing collagen. This phenomenon is also illustrated in Figs. 9 and 10 (group VI). Increased numbers of lymphocytes were present in the stroma (Fig. 4). These forms of cellular activity were particularly common beneath areas of drusen and basal laminar deposit (BLD) formation.

In the example of the atrophic form (Fig. 5) a giant cell is shown, at the light microscope level, closely associated with the inner surface of Bruch's membrane. The single-cell nature of the giant cell was confirmed by electron microscopy. It is surrounded by degenerated pigmented material and is accompanied by an inflammatory infiltrate in the choroid. Inflammatory cells were observed enveloping-long spacing collagen associated with the outer surface of Bruch's membrane; no breaks in the membrane were found. An example of the disciform end stage of SMD is shown at the light microscope level in Fig. 6. A series of breaks in Bruch's membrane have developed and a choroidally derived new vessel is apparent in association with fibroplasia and haemorrhage in the outer retinal layers. An ultrastructural view of the new vessel tip is shown in Fig. 7. New vessels were frequently found to be surrounded by fibrous tissue (Fig. 8). Macrophage-series cells and lymphocytes were observed in close proximity to the outer surface of Bruch's membrane (Fig. 9). Macrophages were frequently observed engulfing long-spacing collagen in this region. Figure 10 is a higher magnification view of Fig. 9 and illustrates the engulfment of both long-spacing collagen

Fig. 7. An electron micrograph of the new vessel (*NV*) shown in Fig. 6. Red blood cells (*RBC*) are apparent within the lumen of the new vessel. *E* indicates an endothelial cell nucleus in the tip of the vessel above Bruch's membrane (*B*). (×1,194 final magnification)

Fig. 8. From the same specimen as the previous two examples, close to the fibrous tissue seen in Fig. 2. A layer of neovascular fibrous tissue (*NVF*) is situated between the remains of the *RPE* (*RPE*↔) photoreceptors (↓*P*) and Bruch's membrane (*B*). A red blood cell (↓*RBC*) and a monocyte (*M*) are apparent within the lumens of the new vessels (*E* indicates endothelial cell nucleus). The new vessels are surrounded by collagen fibres (*C*) and fibroblasts (*F*→). (×1,680 final magnification)

Fig. 9. From a group-VI patient illustrating an inter-relationship between Bruch's membrane (*B*), a macrophage with bilobed nucleus (*M*), long-spacing collagen (*LSC*) and a lymphocyte (*L*). Long-spacing collagen is also present above Bruch's membrane. (×4,500 final magnification)

Fig. 10. Higher magnification view of Fig. 9. Two types of collagen are partially engulfed by the macrophage (*M*), long-spacing collagen (*LSC*) and collagen fibrils (*CF*). (×18,840 final magnification)

Fig. 11. This figure shows a multinucleate giant cell (*G*) lying above Bruch's membrane (*B*). A neovascular complex (*NVC*) has developed between the remains of the RPE, associated BLD and the giant cell. Bruch's membrane immediately below the giant cell is reduced in thickness. The specimen is from a group-VI patient and illustrates the close association between chronic inflammatory cells and neovascularisation in the disciform response. (×1,960 final magnification)

Fig. 12. Taken from an 82-year-old patient with disciform degeneration, the figure shows epitheloid cells (*E*) between Bruch's membrane (*B*) and the remains of the RPE. These cells are often associated with collagen formation (*C*) and fibroblasts (*F*). (×1,680 final magnification)

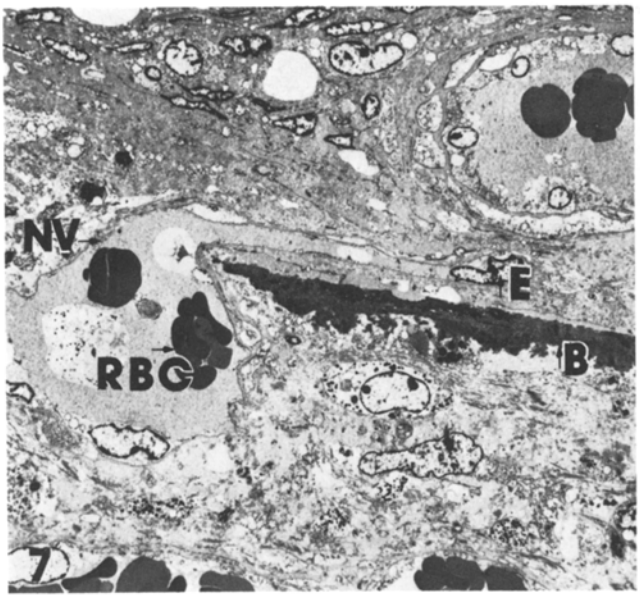
NV
E
RBC
B
7

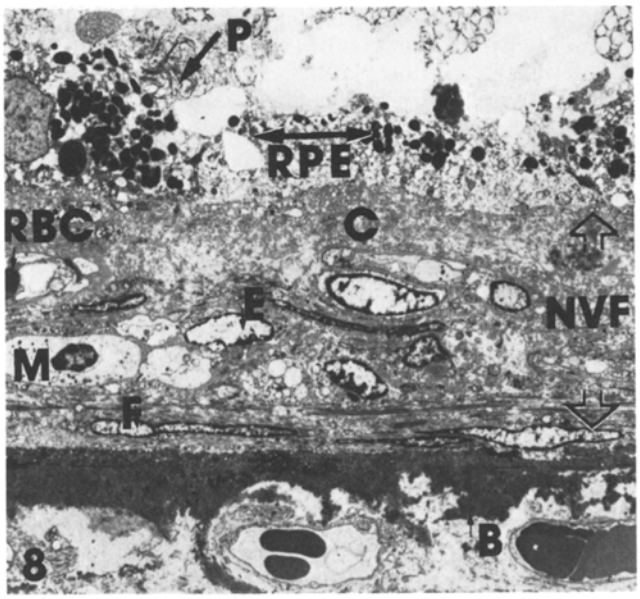
P
RPE
RBC
C
NVF
E
M
F
B
8

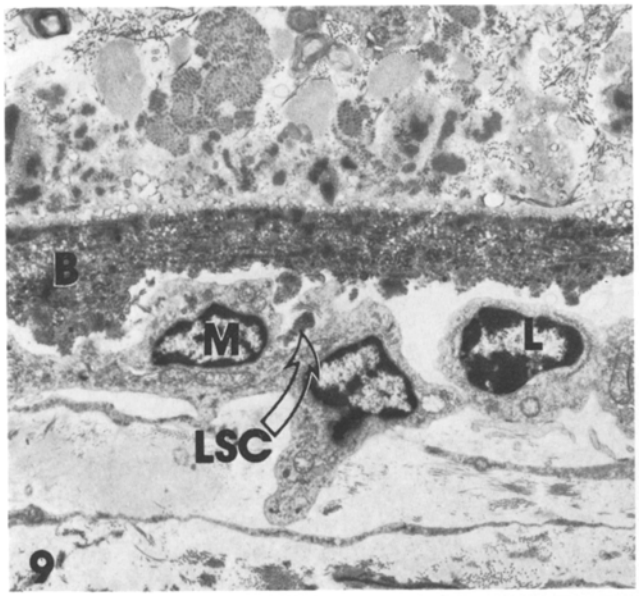
B
M
L
LSC
9

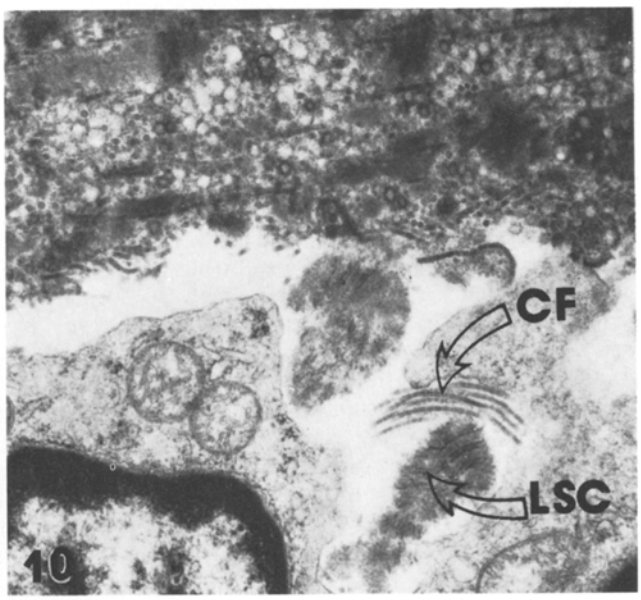
CF
LSC
10

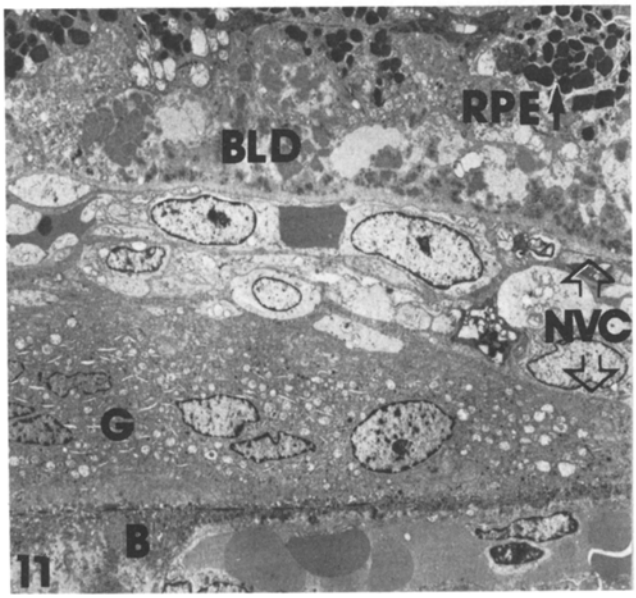
RPE
BLD
NVC
G
B
11

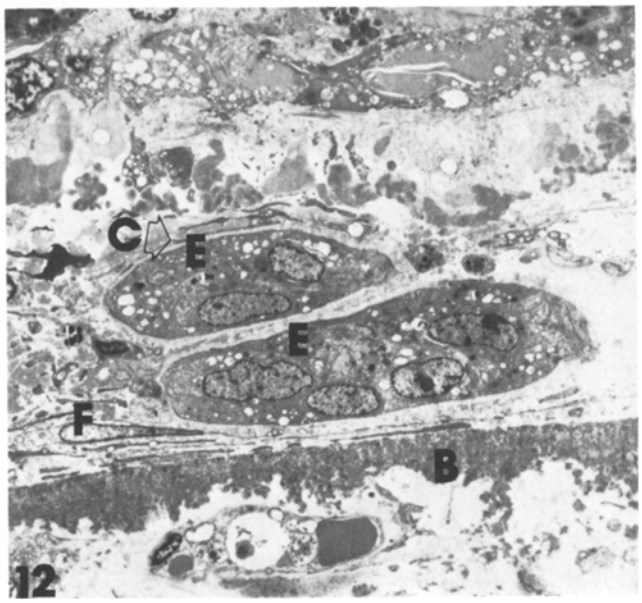
C
E
E
F
B
12

and collagen fibrils. In a previous paper (Penfold et al. 1984), more numerous examples of the association of lymphocytes, macrophages, fibroblasts and mast cells with the formation of breaks in Bruch's membrane were presented. Figure 11 shows a giant cell closely applied to Bruch's membrane in association with a neovascular complex. Epitheloid cells were also observed in areas of active neovascularisation and fibroplasia (Fig. 12).

Estimates were made of the frequency of occurence of giant cells in active end-stage eyes processed for electron microscopy. Of 11 disciform eyes from 8 patients, 7 eyes had giant cells. Of 5 geographic atrophy eyes from 4 patients, 4 had giant cells. These figures suggest that giant cells are commonly involved in both forms of end stage disease. The possible inter-relationships between inflammatory cells, neovascularisation and fibroplasia is considered in the discussion.

The cell counts presented in Table 1 indicate a progressive increase in cell numbers at the macular from group I through group VI in both the underlying stroma (s) and in close proximity to Bruch's membrane (ss). The One-Way Analysis of Variance statistical test was conducted to assess the overall significance of the counts (Table 2). Although there is a large standard deviation for some of the groups, the analysis of variance procedure accommodates within-group variability by incorporating this factor in the error term. The One-Way Analysis of Variance was significant ($F=3.42$, $P<0.01$) and justified subsequent comparisions between group means using the Sheffé test (Table 3). For this purpose cells in the stroma (s) and in the superficial stroma (ss) were added together. The results show that there was a significant increase in cell numbers between normal eyes (group I) and disciform eyes (group VI), normal eyes and atrophic eyes (group V), and normal eyes and intermediate phases (groups II–IV). These results are comparable to those of a previous study using 0.5-μm sections (Penfold et al. 1984).

Statistical analysis of the correlation co-efficient (r) between cells in the stroma (ss+s) and cells in the blood vessels (c+cc) for each group gave the following results: group I, $r=0.039$, $P=<0.1$; group II, $r=0.78$, $P=<0.01$; group III, $r=0.31$, $P=<0.1$; group IV, $r=0.55$, $P=<0.05$; group V, $r=0.21$, $P=<0.1$; group VI, $r=0.15$, $P=<0.1$. The results indicate that a significant relationship ($r=0.78$, $P=<0.01$) existed between numbers of cells in the stroma and numbers of cells in the blood vessels in group II. There was a small degree of correlation between stromal and vascular cells in group IV and almost none in groups I, III, V and VI.

Table 2. One-Way Analysis of Variance

Source	Sums of *squares*	*df*	Mean *squares*	*F*
No. of stromal cells	32,428	5	6,485.6	3.42*
Error	215,956	114	1,894.35	
Total	248,384	119		

* $P<0.01$

Table 3. Summary table for significant differences between sample means using Scheffé test

Groups		1	2,3,4	5	6
	$\bar{x}$	14.65	52.8	47.9	68.65
1	14.65	–	*	*	**
2,3,4	52.8		–	NS	NS
5	47.9			–	NS

* $P<0.05$ ** $P<0.01$

NS = Not significant; $\bar{x}$ = mean of ss+s

Discussion

Low-grade chronic inflammation is associated with some of the most common disabling diseases of man. Its typical features include the recruitment and proliferation of immunocompetent cells, primarily of the macrophage-monocyte series. It is often associated with fibroplasia and vascular proliferation. Some stimuli evoke a distinctive pattern of response referred to as granulomatous inflammation (Robbins and Cotran 1979; Boros 1978). A granuloma may be defined as a chronic inflammatory reaction containing a predominance of cells of the mononuclear phagocyte series (MPS), including giant cells and epitheloid cells (Turk 1980). The present findings demonstrate the involvement of chronic inflammatory cellular components in early, intermediate and late phases of senile macular degeneration.

Early degenerative changes (group II) are associated with the formation of a deposit beneath the pigment epithelium referred to as BLD (Sarks 1976). At the ultrastructural level the deposit contains structures resembling long-spacing collagen described by Hogan et al. (1971) and Ghadially (1982). We have shown in this paper that increasing numbers of inflammatory cells are found in both the choroidal stroma and blood vessels in association with these changes (Tables 1–3). Calculation of the correlation co-efficient ($r=0.78$, $P<0.01$) between cells in the stroma and cells in the blood vessels showed a high correlation factor for these figures only in the early stages of the disease (group II). No significant relationship existed between cells in the stroma and cells in the vasculature in the controls (group I). One possible explanation would be that these findings reflect a process of active recruitment of inflammatory cells from the vasculature into the stroma. The existance of a possible causal relationship between early degenerative changes and the inflammatory infiltrates is still under consideration.

Fig. 13. Taken from a 6-μm wax section, this figure illustrates the appearance of a giant cell (↑*G*) in a group-V patient. These cells were frequently associated with the advancing edge of the atrophic process (*A*↑); RPE indicates the retinal pigment epithelium. (×343 final magnification)

Figs. 14. and 15. Taken from the same specimen, these figures illustrate the level of detail available for the purposes of cell counts presented in the results. *IVL* indicates intravascular leucocytes, *EVL* extravascular leucocytes, *RBC* red blood cells. (×550 final magnification)

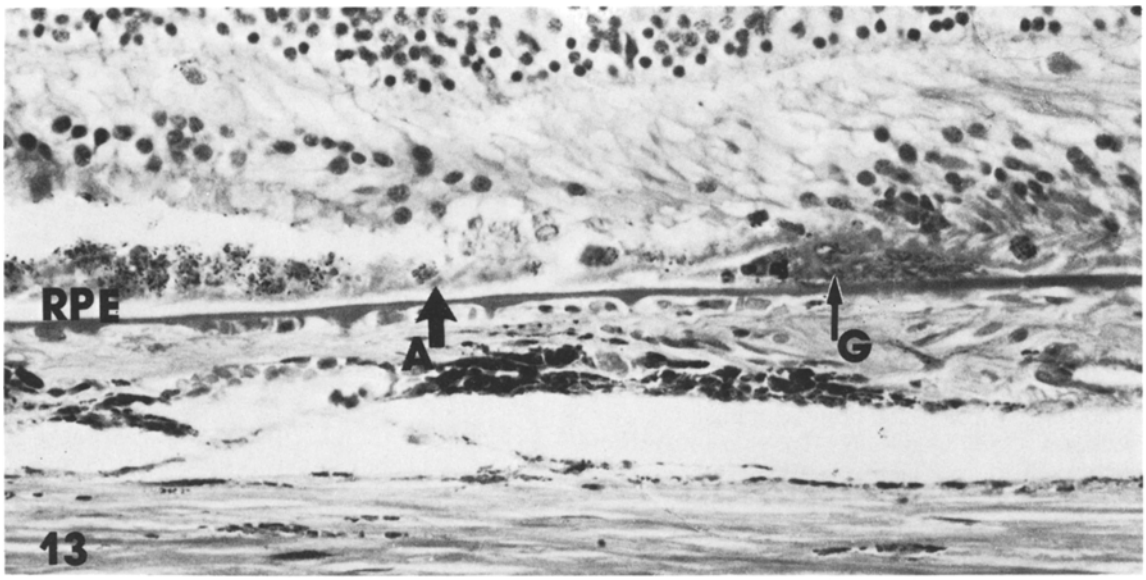
RPE
A
G
13

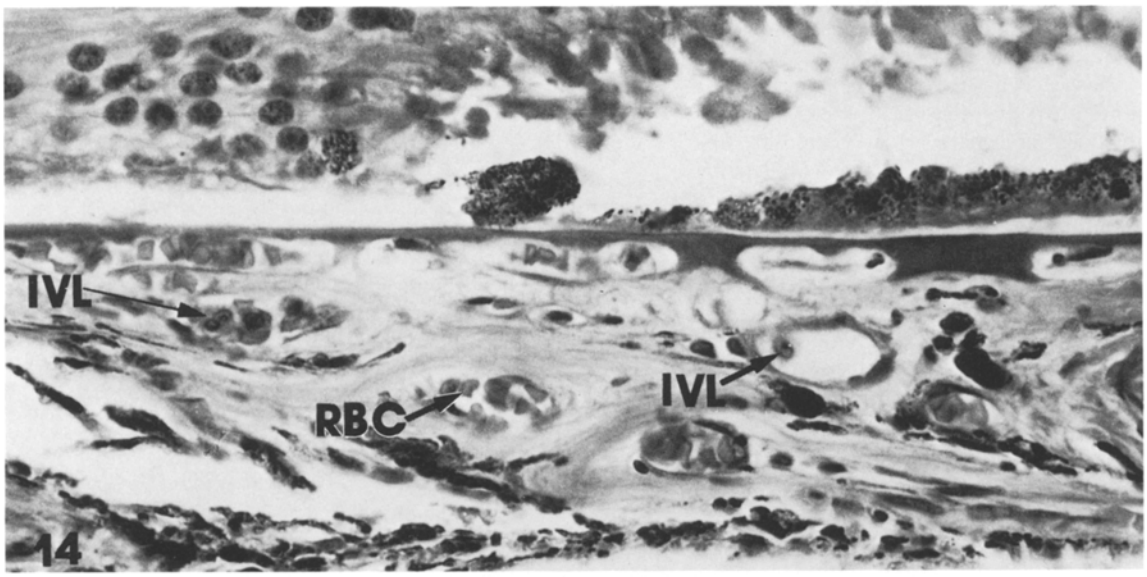
IVL
RBC
IVL
14

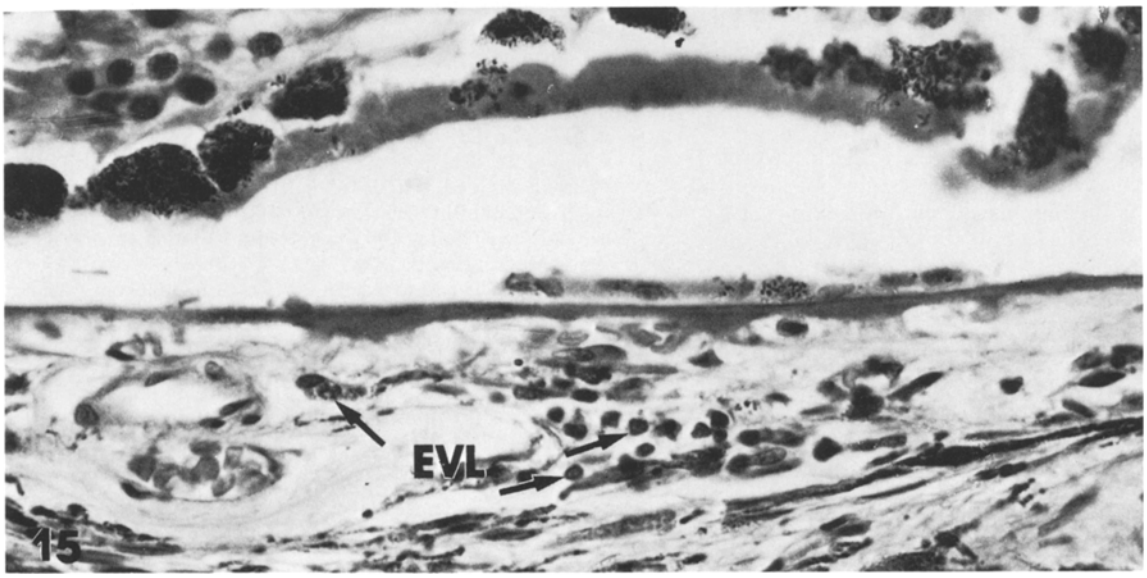
EVL
15

Intermediate phases of macular degeneration (groups III and IV) are characterised by thickening of the BLD and breakdown of drusen (Sarks et al. 1984, in press). The results of the cell counts (Tables 1–3) and calculation of the correlation co-efficient suggest that active recruitment of cells from the vasculature does not occur to the same extent during this phase of the disease. However, the appearance of lymphocytes, macrophages and fibroblasts in the stroma (Figs. 3 and 4) suggests that an inflammatory response is in progress. The observation of monocytes and fibroblasts apparently enveloping long-spacing collagen (Fig. 8) raises the possibility that the collagen or another abnormal constituent of Bruch's membrane is the focus of this response.

Two forms of end-stage SMD have been identified (Sarks 1980). The disciform response typically involves pigmentary disturbances of the RPE, softening of drusen, penetration of Bruch's membrane by choroidal new vessels and fibroplasia. The atrophic form is associated with decreasing numbers of hard drusen and the formation of areas of degeneration of the RPE in the absence of neovascularisation. Both forms of end stage involve increased numbers of inflammatory cells in the stroma, including giant cells and MPS cells. These types of cells are classically associated with a chronic inflammatory response to a poorly degradable stimulus. Giant cells have been observed closely applied to both the internal and external surface of Bruch's membrane, indicating that a constituent of the membrane may provide the inflammatory stimulus. Giant cells and monocytes have also been noted closely related to neovascular membranes (Fig. 12), and epitheloid cells were found in areas of neovascularisation and fibroplasia. It has been pointed out elsewhere (Turk 1980) that epitheloid cells contain rough endoplasmic reticulum and could secrete factors which stimulate fibrosis. These observations may also be related to reports in which factors derived from lymphocytes (Postlethwaite et al. 1976; Wahl et al. 1978) and activated macrophages in vitro (Polverini et al. 1977; Benezra 1978; DeLustro et al. 1980; Martin et al. 1981) have been implicated in fibroblast and new blood-vessel proliferation.

In a previous publication we showed that leucocytes and fibroblasts played a role in the formation of breaks in Bruch's membrane (Penfold et al. 1984). Here we have shown that the role of immunocompetent cells may be extended to include their involvement in early, intermediate and late phases of chronic inflammation during the course of SMD. At this stage it is not possible to decide whether these cells represent a response to existing degenerative changes, or whether they act as essential mediators of degeneration and neovascularisation. Although the cell counts presented here demonstrate that the diseased stroma contains more inflammatory cells than the normal stroma, we would refrain from detailed conclusions regarding the possible relationship between cells in the stroma, cells in the vasculature and their relationship to the stage of the disease. We would suggest, however, that our results imply that the pathogenesis of SMD involves a low-grade chronic inflammatory response focused about Bruch's membrane.

Acknowledgements. The authors wish to thank Professor A.W.J. Lykke and Dr. M.R. Dickson for the provision of facilities in the Biomedical Electron Microscope Unit, University of New South Wales. We also wish to acknowledge the support of Dr. G.W. Carter, Medical Superintendant of Lidcombe Hospital, New South Wales. Thanks are also due to Mr. F. Cutajar for technical assistance and to Miss Anne Healy for typing the manuscript. Special thanks are due to Dr. R. Mitchell for his assistance with the statistical analyses. This work was supported by a grant from the National Health and Medical Research Council of Australia.

References

Benezra D (1978) Neovasculogenic ability of prostaglandins, growth factors and synthetic chemo-attractants. Am J Ophthalmol 86:455

Boros DL (1978) Granulomatous inflammation. Prog Allergy 24:183

DeLustro F, Sherer GK, LeRoy EC (1980) Human monocyte stimulation of fibroblast growth by a soluble mediator(s). J Reticuloendothel Soc 28:519

Ghadially FN (1982) Ultrastructural pathology of the cell and matrix, 2nd edn. Butterworths, Sydney

Ghafour IM, Allan D, Foulds WS (1983) Common causes of blindness and visual handicap in the west of Scotland. Br J Ophthal 67:289

Grindle JFC, Marshall J (1978) Ageing changes in Bruch's membrane and their functional implications. Trans Ophthalmol Soc UK 98:172

Hogan MJ, Alvarado JA, Weddell JE (1971) Histology of the human eye: An atlas and textbook. Saunders, Philadelphia

Killingsworth MC, Sarks SH (1982) Giant cells in disciform macular degeneration of the human eye. Micron 13:359

Lancet Editorial (1983) Lancet 1:278

Martin BM, Gimbrone MA, Unanue ER, Cotran RS (1981) Stimulation of nonlymphoid mesenchymal cell proliferation by a macrophage-derived growth factor. J Immunol 126:1510

Penfold PL, Killingsworth MC, Sarks SH (1984) An ultrastructural study of the role of leucocytes and fibroblasts in the breakdown of Bruch's membrane. Aust J Ophthalmol 12:23

Polverini PJ, Cotran RS, Gimbrone MA, Unanue ER (1977) Activated macrophages induce vascular proliferation. Nature 269:804

Postlethwaite AE, Snyderman R, Kang AH (1976) The chemotatic attraction of human fibroblasts to a lymphocyte-derived factor. J Exp Med 144:1188

Robbins SL, Cotran RS (1979) Pathologic basis of disease, 2nd edn. Saunders, Philadelphia

Sarks SH (1976) Ageing and degeneration in the macular region: a clinicopathological study. Br J Ophthalmol 60:324

Sarks SH (1980) Drusen and their relationship to senile macular degeneration. Aust J Ophthalmol 8:117

Sarks SH, Van Driel D, Maxwell L, Killingsworth MC (1980) Softening of drusen and subretinal neovascularisation. Trans Ophthalmol Soc UK 100:414

Sarks SH, Penfold PL, Killingsworth MC, Moussa AY (1984) Drusen and their relationship to choroidal neovascularisation. Excerpta Medica (in press)

Sorsby A (1966) The incidence and causes of blindness in England and Wales 1948–1962. Rep Health Soc Subj (Lond) 144:14

Turk JL (1980) Immunologic and non-immunologic activation of macrophages. J Invest Dermatol 74:301

Wahl SM, Wahl LM, McCarthy JB (1978) Lymphocyte-mediated activation of fibroblast proliferation and collagen production. J Immunol 121:942

Received December 27, 1983